ACS Macro Letters

Letter

pubs.acs.org/macroletters

Rayleigh Instability Induced Cylinder-to-Sphere Transition in Block Copolymer Micelles: Direct Visualization of the Kinetic Pathway

Lulu Wang,[†,‡] Haiying Huang,*[,†,‡] and Tianbai He*[,†,‡]

[†]State Key Laboratory of Polymer Physics and Chemistry, Changchun Institute of Applied Chemistry, Chinese Academy of Sciences, Changchun 130022, P. R. China

[‡]Graduate School of the Chinese Academy of Sciences, Beijing 10039, P. R. China

Supporting Information

ABSTRACT: Direct visualization of morphological evolution remains extremely challenging despite its critical importance to understand the basic fundamentals behind the transition. Here we report on the detailed observation of a spontaneous cylinder-to-sphere morphological transformation of amphiphilic poly(2-vinylpyridine)-*b*-poly(ethylene oxide) (P2VP-*b*-PEO) diblock copolymer micelles in aqueous solution, which first provides experimental evidence that the fragmentation pathway is driven by Rayleigh instability showing the distinctive signatures during the transition. Owing to the instability of cylindrical micelles and the fluidity of micellar cores, our results show that the cylindrical micelles spontaneously undulate and transform into spherical micelles through distinct intermediate states, including undulated cylinders and pearl-necklace-like micelles with a perfect sinusoidal wave throughout the length. Moreover, the present system with transitional morphology is proved to be able to act as a model to encapsulate hydrophobic guests in the micellar cores, which displays a relatively sustained release behavior. The specific kinetic pathway provides new insight into the mechanism of block copolymer micellar morphological transition; meanwhile, the dynamic system might serve as a promising candidate for unique nanostructure design as well as contribute to the transition-coupled guest delivery and controlled release.

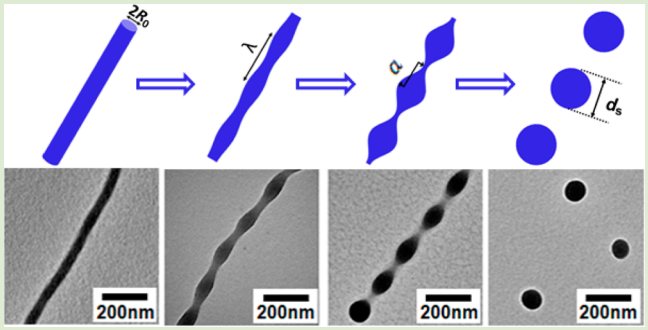

Block copolymers can spontaneously self-assemble in selective solvent to form micelles of various morphologies.[1−4] Due to the higher molecular weight and slower chain dynamics, the micellization behavior of amphiphilic block copolymers is much more complicated than that of low molecular weight surfactants.[5,6] Even if the equilibrium state is predictable, these materials are prone to be trapped kinetically in nonequilibrium states, which depend sensitively on the preparation procedures.[7−11] In consideration of the nonergodic process, it is essential to understand the underlying mechanism and kinetic pathway of the morphological transition from one state to another in block copolymer micellar systems. However, to date, real-time monitoring of the transformation process remained a challenging task mainly due to the fast structural change and narrow time window of detection. Only a few researches have experimentally showed the details involved in the transitions, despite their critical importance for identifying the different evolutionary path and self-assembly behavior.[12−16]

Here, we are particularly interested in the morphological transitions of cylindrical micelles to spherical micelles, focusing on the fragmentation pathways driven by Rayleigh instability. In the past two decades, the transition paths of cylinders to spheres have been widely investigated both theoretically and experimentally. In the pioneering work reported by Eisenberg, the transition path of cylinders to spheres has been identified as a process that bulbs develop on either or both ends of cylinders and then pinched off to release free spheres.[17] Later, Discher and co-workers extended the theory and reported that a long and flexible cylinder fragmentized segmentally into shorter ones, whereas short cylinders pinched off from the end and eventually broke further into spherical micelles.[18−20] On the other hand, Grason and Santangelo developed a mean-field model for diblock copolymer micelles, indicating that a metastable undulated cylinder morphology prevails during cylinder-to-sphere transition when spherical micelles are preferred in equilibrium.[21] Likewise, in an experiment Jain and Bates reported for the first time a peristaltic morphology with undulations that propagate at a fixed wavelength for three periods away from the spherical terminus of cylindrical micelles, which resemble the well-known Rayleigh instability.[22]

Initially, Rayleigh instability was used to describe the phenomenon of instability of liquid cylinders due to surface tension.[23] The liquid cylinders will break up into droplets with uniform size and regular spacing to decrease the surface area and hence the surface energy. In fact, Rayleigh instability induced transformation is widely observed in a variety of

Received: March 17, 2014
Accepted: April 17, 2014
Published: April 21, 2014

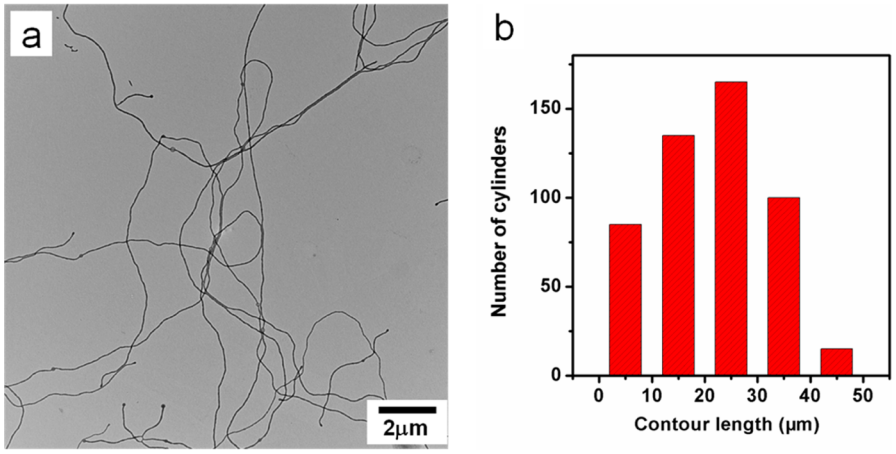

Figure 1. (a) TEM images of long smooth $P2VP_{251}$-*b*-PEO_{134} cylindrical micelles in water measured immediately after evaporation of the chloroform solvent. (b) The contour length distribution of cylindrical micelles was obtained by measuring no less than 500 cylindrical micelles in TEM images.

systems, such as metal nanowires,[24−27] tubular lipid vesicles,[28] polymer nanotubes, and fibers.[29−35] However, in the case of cylinder-to-sphere transition of block copolymer micelles, even though Rayleigh instability is believed to destabilize the system,[20−22] so far no experimental evidence provides full details of such transition; in particular, a well-defined intermediate pearl-necklace-like structure had never been trapped in the transitional process. Yet, the direct visualization of the entire and spontaneous process is crucial to understanding both the distinct pathway and the transition mechanism driven by Rayleigh instability, which is a fundamental issue that has remained ambiguous for decades and lacks direct experimental evidence.

In this study, direct observation of spontaneous morphological transitions of cylindrical micelles to spherical micelles was achieved in the amphiphilic poly(2-vinylpyridine)-*b*-poly(ethylene oxide) ($P2VP_{251}$-*b*-PEO_{134}) diblock copolymer system, which is proved to be exactly in agreement with the Rayleigh instability induced transformation. The initial prepared thermodynamically unstable cylindrical micelles can spontaneously transform to spheres slowly in ca. 10 days, which gives us enough time to precisely monitor and identify the intermediate structures in detail. Cylinders with perfect sinusoidal undulations and pearl-necklace-like structures with uniform particle size and spacing were detected during the transition, which, to the best our knowledge, were revealed exclusively in the present system. Our findings may not only provide a fundamental insight into the mechanism of cylinder-to-sphere transition but also pave the way for rational design and control of the self-assembly of cylindrical micelles, yielding promising new nanostructures.

The pure and long $P2VP_{251}$-*b*-PEO_{134} cylindrical micelles in aqueous solution were prepared through an "emulsification and solvent evaporation" method, which has been recently considered as an effective method to generate amphiphilic polymer micelles.[10,11,19,36−39] The $P2VP_{251}$-*b*-PEO_{134} diblock copolymer was dissolved in a water-immiscible organic solvent (chloroform), and then the polymer solution was dispersed as emulsion droplets in an aqueous phase. Finally the chloroform was allowed to evaporate slowly and completely under vigorous stirring at room temperature, which enabled us to obtain such long and smooth cylindrical micelles consisting of a P2VP core and PEO corona. Figure 1a shows TEM images of the cylindrical micelles in pure water captured immediately after complete evaporation of the chloroform solvent. It is found that the exclusive cylindrical micelles with an average diameter of 43.11 ± 4.33 nm and contour lengths on the order of several tens of micrometers were generated in the system. As shown in Figure 1b, the contour length distribution of such cylindrical micelles was determined by measuring no less than 500 cylindrical micelles in TEM images. On a time scale of days, these cylindrical micelles will spontaneously transform into more stable spherical micelles under continuous mild stirring. It is noteworthy that in our experiment stirring is not a prerequisite for the morphological evolution but can only speed up the transformation process. In controlled experiments without stirring, the cylinders transform into spheres via similar stages in a time period of ca. 2 months. Considering that stirring will exert shearing force, which might affect the micelle formation,[40] a mild stirring rate (300 rpm) was applied after chloroform was removed to avoid any unexpected shearing influence throughout the experiment. Meanwhile, further by employing other traditional micelle preparation methods, we believe that the cylindrical micelles are kinetically trapped structures depending sensitively on the specific emulsification and solvent evaporation process (see details in the Supporting Information, Figure S1). In the following sections, we will focus on the nature of the fragmentation pathways of such cylindrical micelles to access the details involved in the structural evolution.

The time-dependent morphological transition behavior from cylinders to spheres was completed in around 10 days. Before directly visualizing the entire morphology of micelles, a dynamic light scattering (DLS) experiment was performed to in situ characterize the size information on micelles in water. The apparent hydrodynamic diameter (D_h) decreased from 534 to 89 nm as a function of time, which indicates the significant trend of spontaneous fragmentation of long cylinders (Supporting Information, Figure S2). In a corresponding manner, representative TEM images show that $P2VP_{251}$-*b*-PEO_{134} cylindrical micelles spontaneously transform to spherical micelles with time in water (Figure 2). As described, the cylindrical micelles possess a smooth surface at the beginning of the morphological evolution (Figures 1a and 2a), which becomes undulated within hours (Figure 2b). One can see pronounced undulations along the cylinders in the high magnification TEM images taken after 2 h (inset of Figure 2b). We also found that the undulations could start from both ends

dx.doi.org/10.1021/mz500158f | *ACS Macro Lett.* 2014, 3, 433−438

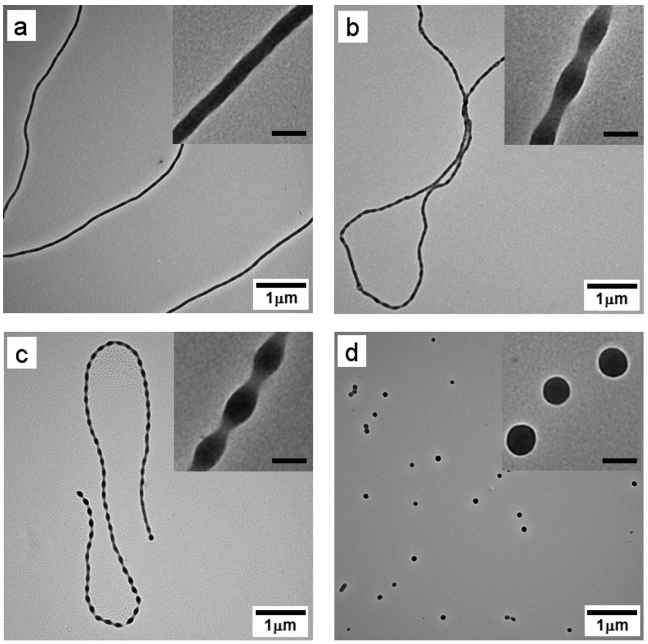

Figure 2. TEM images of $P2VP_{251}$-*b*-PEO_{134} cylindrical micelles spontaneously transform to spherical micelles with time in water. The images were taken during the transition after (a) 0 h, (b) 2 h, (c) 5 days, and (d) 10 days, respectively, when no chloroform was visible. Insets show the high-magnification TEM images of corresponding morphology, and the scale bar in the insets represents 100 nm.

of the cylinder or randomly "budding" in the center, and cylinders with local undulation parts could also be observed at this stage (Supporting Information, Figure S3). Stirring overnight was long enough to transform nearly all the smooth cylinders into pearl-necklace-like micelles, which could maintain the morphology for days and were evidently displayed in Figure 2c (see also Supporting Information Figure S4 for large scale of pearl-necklace-like micelles at lower magnification). Strikingly, the strong beadlike deformations lead to the formation of a necklace-like configuration with perfect sinusoidal profile. Most importantly, such unique features are obviously throughout the length of the cylinders. The pearl-necklace-like micelles can maintain their morphology for several days because the process of approaching spherical micelles is sufficiently slow. As shown in Figure 2d, spherical micelles have dominant morphology after 10 days. Given enough time, all the cylindrical micelles eventually transform into spherical micelles with an average diameter of 82.41 ± 9.88 nm as measured from such TEM images.

There are two noteworthy features during the cylinder-to-sphere transition. One key feature is that the whole morphological transition process is identified unambiguously within the time scale of experimental observation, which is of critical importance for understanding the kinetic pathway and transition mechanism. As mentioned above, a sphero-cylinder (cylindrical body with enlarged spherical end-caps at the terminus) mediated transition mechanism has been widely accepted.[17−20] Very recently, an undulated ribbon structure has also been hypothesized to develop spherical end-caps and further split off separated spheres considering dimensions of the two structures, although the dynamic process was not observed.[41] Reversely, a different perspective has also been proposed that the transformation from cylinders proceeded directly to spheres without any intermediate structures on the millisecond range.[42] However, in our system, it is shown that the morphological transition definitely passed through several stages with obvious characteristic intermediate states, which completed in a relatively long time (ca. 10 days). It is likely that the great difference in transition kinetics is related to the driving force of morphological transition, in other words, the degree of deviation from equilibrium. In previous work, the cylinder-to-sphere morphological transitions of block copolymer micelles usually mutated as a result of an external stimulus, such as a jump in solvent composition,[17,42] pH, ionic strength,[18] as well as change in polymer chain structure.[19] Nevertheless, the situation in the present system is different because the cylindrical micelles spontaneously transform into spheres without an additional disturbance, indicating an intrinsic driving force associated with the kinetically trapped but not frozen cylindrical structure. On the other hand, it was found that the cylinders become undulated in hours, while the complete rupture of the undulated ones would cost several days. From the energetic perspective, the initial smooth cylinders are thermodynamically unstable states that lie far away from equilibrium, which tend to undulate quickly. In comparison, the undulated cylinders are metastable and might need a longer time to cross over a free energy barrier to reach the final stable states.[43]

The other attractive feature during transition is the formation of uniform pearl-necklace-like micelles with Rayleigh instability induced undulations throughout the length. Only a few studies report the analogous pearl-necklace-like structures, which mainly reflected blending induced locally unfavorable energetic interaction[8,38] or frustrated sphere-to-cylinder transition.[17,44] Wooley et al. also trapped pearl-necklace-like morphology as intermediate structures in the cylinder-to-sphere transition, where bulbs were randomly formed along the rods.[45] However, the pearl-necklace structure profile in their work is essentially different from the sinusoidal one induced by undulation of cylinders, since the cross-linking reactions facilitated kinetic trapping of assemblies, which is irrelevant to Rayleigh instability induced transformation. On the other hand, we note that the Rayleigh instability resulted transition mechanism has previously been proposed for surfactant cylindrical micelles based on computer simulations and calculations.[46,47] Besides, similar undulation induced cylinder-to-sphere phase transition were also reported in block copolymer melts.[48−50] So far, in block copolymer micellar systems, Rayleigh instability induced beadlike deformations were observed only near the ends of cylinders but could proceed along very limited periods and appear to be damped in the long central portions.[13,22] Compared with previous observations, the well-defined structure with perfect sinusoidal wave spreading all over the length obtained here should be the only currently known Rayleigh instability induced pearl-necklace-like intermediate in the block copolymer micellar system.

More importantly, as typical signatures of Rayleigh instability, both the undulated cylinder and pearl-necklace-like intermediate structure indicated that a mechanism resembling the Rayleigh instability triggered the morphological transition from cylinder to sphere. To get better insight into this transformation, we further compare the experimentally measured characteristic sizes with the theoretical calculated values based on Rayleigh instability, which are listed in Table 1. According to the work of Nichols and Mullins,[51] who applied the Rayleigh instability type transformation to solid cylinders, a

dx.doi.org/10.1021/mz500158f | *ACS Macro Lett.* 2014, 3, 433−438

Table 1. Comparison between the Experimental Values and the Theoretical Values Based on Rayleigh Instability

characteristic parameters	$2R_0$[a] [nm]	λ_{min}[b] [nm]	λ_{max}[c] [nm]	d_s[d] [nm]
theoretical value	43.11	135.37	191.62	81.48
experimental value	43.11	—	184.99	82.41
standard deviation[e]	4.33	—	12.30	9.88

[a]Radius of the initial smooth cylinder. We assume that the theoretical value is equal to the experimental value. [b]Critical wavelength for cylinder to break down. [c]Perturbation of wavelength at maximum growth rate. [d]Diameter of spheres. [e]Calculated from no less than 500 measurements.

cylinder with isotropic surface energy is analyzed with respect to variations of the radius r by surface undulation of the form

$$r = R_0 + a \sin \frac{2\pi}{\lambda} x$$

where R_0 is the radius of the initial smooth cylinder; a is the amplitude of the perturbation; λ is the wavelength of the perturbation; and x is the coordinate along the cylindrical axis. A schematic illustration of the transformation pathway from cylindrical micelles to spherical micelles driven by Rayleigh instability is presented in Figure 3. The critical wavelength for

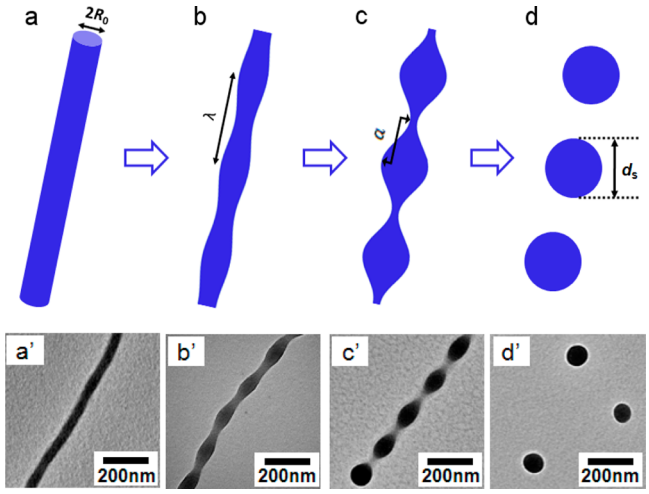

Figure 3. Schematic illustration and corresponding TEM images of the transformation pathway from cylindrical micelles to spherical micelles driven by the Rayleigh instability, where R_0 is the radius of the initial smooth cylinder, a the amplitude of the perturbation, λ the wavelength of the perturbation, and d_s the diameter of spheres. (a) Smooth cylinders; (b) undulated cylinders; (c) pearl-necklace-like structures; (d) spheres.

cylinders to break down is estimated by $\lambda_{min} = 2\pi R_0$. As long as λ is larger than the circumference of the cylinder ($\lambda > \lambda_{min}$), the amplitude increases spontaneously, and a cylinder will become unstable against the sinusoidal perturbations. If the wavelength reaches the maximum point, $\lambda_{max} = 2\pi\sqrt{2}R_0 = 8.89R_0$, the perturbations would grow fastest. The amplitude of the perturbation with the maximum growth rate continues to increase, and the cylinders eventually break up into spheres with an estimated diameter $d_s = 3.78R_0$. Here, taking $2R_0$ = 43.11 nm as measured from TEM images (Figure 3a, a′), we can calculate that λ_{min} = 135.37 nm, λ_{max} = 191.62 nm, and d_s = 81.48 nm, respectively. When compared with the experimentally measured wavelength (the distance between the corresponding points of two consecutive undulations) of the metastable undulating cylinders 184.99 ± 12.30 nm, it is reasonable to expect that the smooth cylindrical micelles are destabilized by Rayleigh instability (Figure 3b, b′). With time the undulation amplifies, and the wave grows in amplitude, resulting in the formation of well-defined pearl-necklace-like structure (Figure 3c, c′). Further undulation then leads to fragmentation into spherical micelles with radius of 82.41 ± 9.88 nm, which also agrees well with the theoretically predicted value d_s = 81.48 nm (Figure 3d, d′). The above results positively demonstrate that the fragmentation pathway of cylindrical micelles is in strict conformity with Rayleigh instability.

Notwithstanding the evidence that Rayleigh instability is the dominant driving force in the whole cylindrical-to-spherical micellar transition, the underlying physics involved is actually different. It is known that the Rayleigh instability is driven by the surface energy of a fluid cylinder; however, the free energy of block copolymer micelles is governed by three different components, i.e., the stretching energy of core blocks, repulsion of the corona chain, and surface tension.[1] On the basis of the experimental evidence, we consider the transformations to be predominantly driven by the interface energy that relates to the surface tension between the core-forming blocks and the solvent in the current system. The long cylindrical micelles are temporarily trapped by the unique preparation procedure, but spheres with lower surface energy are much more thermodynamically favorable than cylinders in the given conditions. In addition, we suspect that the composition of the block copolymer P2VP$_{251}$-*b*-PEO$_{134}$ (volume fraction for P2VP blocks is about 81.5%) should be near the cylinder/sphere phase boundary in the phase diagram because we have further attempted to use the block copolymer with different compositions to repeat the procedure, and only spherical micelles could be observed when the core block volume fractions lie in the sphere-forming region far away from the phase boundary (data not shown). The "emulsification and solvent evaporation" method can produce an instantaneous local excess concentration of polymer molecules upon abrupt burst from the chloroform droplets. When the free chains get together quickly to form temporal micelles, cylindrical micelles with more stretched core blocks are favored instead of spherical ones at the very beginning.[52] Ultimately, thanks to the chain mobility of the slightly swollen P2VP cores, the system was allowed to transform slowly on a time scale of days. On the basis of these considerations, we suggest that such a morphological transition only occurs in limited systems depending on the composition of the block copolymer and fluidity of micellar cores, which are indispensible for the spontaneous cylindrical to spherical micellar transformation induced by Rayleigh instability.

By taking advantage of the slow kinetics of morphological evolution in aqueous media, the encapsulation and transition-coupled release behavior of the present system were also examined. When block copolymer micelles are used in guest delivery, morphology transition shows an impact on the loading capacity,[53] and the transition dynamics are related to the rate of release.[54,55] The slow morphological evolution of P2VP$_{251}$-*b*-PEO$_{134}$ micelles in aqueous media described above provides a broad time window for the investigation of such a dynamic process. As a proof of principle experiment, a kind of hydrophobic fluorescent dye Nile Red (NR) was chosen to load into the hydrophobic core domain. The color of micellar

dx.doi.org/10.1021/mz500158f | ACS Macro Lett. 2014, 3, 433−438

solutions turned from bluish-white to pink after introduction of NR, and the successful encapsulation was further confirmed by laser scanning microscopes (LSMs) and fluorescence emission spectra. As seen in LSM images (Figure 4a–d), the

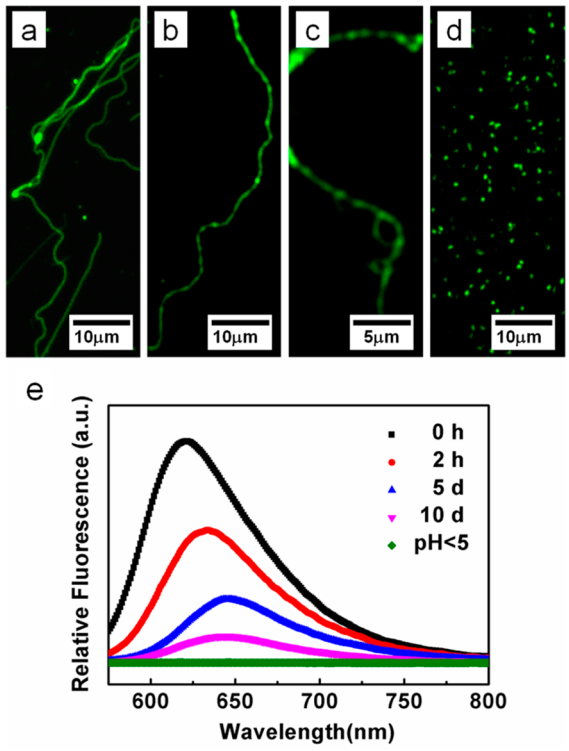

Figure 4. Representative LSM images of Nile Red loaded $P2VP_{251}$-*b*-PEO_{134} micelles in the dynamic process of morphological evolution observed (a) as soon as no chloroform was visible and after (b) 2 h, (c) 5 days, and (d) 10 days, respectively. (e) Fluorescence emission spectra of the micelle solution at different evolution time and after pH-triggered release of NR (λ_{ex} = 550 nm), showing a decrease and red-shift of fluorescence emission due to release of NR molecules to water.

introduction of 1 wt % (relative to $P2VP_{251}$-*b*-PEO_{134}) NR had no obvious influence on the micellar morphological evolution pathway, which provides complementary evidence in aqueous solutions to further prove the in situ micellar morphological transition. Upon excitation at 550 nm, the hybrid micellar solutions exhibited apparent fluorescence emission peaks, which shifted from 621 to 645 nm with a decrease in intensity to about 20% of the initial level in the Rayleigh instability induced morphology transition process (Figure 4e). It is well-known that the fluorescence properties of NR highly depend on the polarity of the probe environment,[56,57] so we can infer that accompanied by the micellar transformation the entrapped NR molecules were released from the hydrophobic medium (P2VP cores) into aqueous solution and quenched. Furthermore, in light of the pH-dependent solubility of P2VP blocks in water (with a pK_a of 5.9), an instantaneous release of NR could be triggered upon lowering the pH value below 5, as evidenced by the negligible fluorescence emission. Although it remains to be elucidated further, we envision that micelles of various, continuous variable morphologies in our system might serve as a stimuli-responsive model and allow for the development of guest delivery vehicles.

In conclusion, a spontaneous morphological transition from cylinder to sphere was fully monitored in a diblock copolymer micellar system, which passed through several stages characterized by sinusoidal undulated cylinders and pearl-necklace-like intermediate structures. On the basis of quantitative measurements and comparisons, it is believed that the Rayleigh instability induced mechanism is responsible for the transformation, which has already been proposed but never been unambiguously visualized in a dynamic block copolymer micellar system. Apart from directly visualizing a detailed picture of the kinetic pathway, the block copolymer micelles in evolutional structures can be a promising candidate and model system in guest delivery and controlled release area. Moreover, the possibility to regulate the P2VP block mobility via coordination or cross-link allows facile tuning or even locking the unstable intermediates at different stages, which offer an opportunity to design and produce new novel nanostructures.

■ ASSOCIATED CONTENT

Supporting Information

Experimental details (S1), micelles obtained by different preparation methods (S2), time-dependent hydrodynamic diameter measured by dynamic light scattering (S3), and various intermediate structures captured in the early stage of Rayleigh instability induced transformation (S4). This material is available free of charge via the Internet at http://pubs.acs.org.

■ AUTHOR INFORMATION

Corresponding Authors

*E-mail: hyhuang@ciac.ac.cn (H.Y. Huang).
*E-mail: tbhe@ciac.ac.cn (T.B. He).

Notes

The authors declare no competing financial interest.

■ ACKNOWLEDGMENTS

This work was supported by the National Natural Science Foundation of China (Grant 21104079 and 21274148).

■ REFERENCES

(1) Cameron, N. S.; Corbierre, M. K.; Eisenberg, A. *Can. J. Chem.* **1999**, *77*, 1311–1326.
(2) Riess, G. *Prog. Polym. Sci.* **2003**, *28*, 1107–1170.
(3) Gohy, J. F. *Adv. Polym. Sci.* **2005**, *190*, 65–136.
(4) Mai, Y.; Eisenberg, A. *Chem. Soc. Rev.* **2012**, *41*, 5969–5985.
(5) Jain, S.; Bates, F. S. *Science* **2003**, *300*, 460–464.
(6) Choi, S.-H.; Lodge, T. P.; Bates, F. S. *Phys. Rev. Lett.* **2010**, *104*, 047802.
(7) Pochan, D. J.; Chen, Z. Y.; Cui, H. G.; Hales, K.; Qi, K.; Wooley, K. L. *Science* **2004**, *306*, 94–97.
(8) Cui, H.; Chen, Z.; Zhong, S.; Wooley, K. L.; Pochan, D. J. *Science* **2007**, *317*, 647–650.
(9) Meli, L.; Santiago, J. M.; Lodge, T. P. *Macromolecules* **2010**, *43*, 2018–2027.
(10) Hayward, R. C.; Pochan, D. J. *Macromolecules* **2010**, *43*, 3577–3584.
(11) Wyman, I.; Njikang, G.; Liu, G. *Prog. Polym. Sci.* **2011**, *36*, 1152–1183.
(12) Hu, J.; Njikang, G.; Liu, G. *Macromolecules* **2008**, *41*, 7993–7999.
(13) Fernyhough, C.; Ryan, A. J.; Battaglia, G. *Soft Matter* **2009**, *5*, 1674–1682.
(14) Denkova, A. G.; Mendes, E.; Coppens, M.-O. *Soft Matter* **2010**, *6*, 2351–2357.
(15) Han, D.; Li, X.; Hong, S.; Jinnai, H.; Liu, G. *Soft Matter* **2012**, *8*, 2144–2151.

(16) Grubbs, R. B.; Sun, Z. *Chem. Soc. Rev.* **2013**, *42*, 7436−7445.
(17) Burke, S. E.; Eisenberg, A. *Langmuir* **2001**, *17*, 6705−6714.
(18) Geng, Y.; Ahmed, F.; Bhasin, N.; Discher, D. E. *J. Phys. Chem. B* **2005**, *109*, 3772−3779.
(19) Geng, Y.; Discher, D. E. *J. Am. Chem. Soc.* **2005**, *127*, 12780−12781.
(20) Loverde, S. M.; Ortiz, V.; Kamien, R. D.; Klein, M. L.; Discher, D. E. *Soft Matter* **2010**, *6*, 1419−1425.
(21) Grason, G. M.; Santangelo, C. D. *Eur. Phys. J. E* **2006**, *20*, 335−346.
(22) Jain, S.; Bates, F. S. *Macromolecules* **2004**, *37*, 1511−1523.
(23) Rayleigh, L. *Proc. London Math. Soc.* **1878**, *10*, 4−12.
(24) Fowlkes, J.; Horton, S.; Fuentes-Cabrera, M.; Rack, P. D. *Angew. Chem., Int. Edit* **2012**, *51*, 8768−8772.
(25) Rauber, M.; Muench, F.; Toimil-Molares, M. E.; Ensinger, W. *Nanotechnology* **2012**, *23*, 475710.
(26) Liao, H. G.; Zheng, H. *J. Am. Chem. Soc.* **2013**, *135*, 5038−5043.
(27) Xu, J.; Zhu, Y.; Zhu, J.; Jiang, W. *Nanoscale* **2013**, *5*, 6344−6349.
(28) Yu, Y.; Granick, S. *J. Am. Chem. Soc.* **2009**, *131*, 14158−14159.
(29) Chen, J. T.; Zhang, M. F.; Russell, T. P. *Nano Lett.* **2007**, *7*, 183−187.
(30) Mei, S.; Feng, X.; Jin, Z. *Macromolecules* **2011**, *44*, 1615−1620.
(31) Chen, D.; Chen, J. T.; Glogowski, E.; Emrick, T.; Russell, T. P. *Macromol. Rapid Commun.* **2009**, *30*, 377−383.
(32) Lee, C. W.; Wei, T. H.; Chang, C. W.; Chen, J. T. *Macromol. Rapid Commun.* **2012**, *33*, 1381−1387.
(33) Fan, P. W.; Chen, W. L.; Lee, T. H.; Chen, J. T. *Macromol. Rapid Commun.* **2012**, *33*, 343−349.
(34) Fan, P. W.; Chen, W. L.; Lee, T. H.; Chiu, Y. J.; Chen, J. T. *Macromolecules* **2012**, *45*, 5816−5822.
(35) Huang, Y. C.; Fan, P. W.; Lee, C. W.; Chu, C. W.; Tsai, C. C.; Chen, J. T. *ACS Appl. Mater. Interfaces* **2013**, *5*, 3134−3142.
(36) Meng, F. H.; Hiemstra, C.; Engbers, G. H. M.; Feijen, J. *Macromolecules* **2003**, *36*, 3004−3006.
(37) Zhu, J.; Hayward, R. C. *Angew. Chem., Int. Ed.* **2008**, *47*, 2113−2116.
(38) Zhu, J.; Hayward, R. C. *J. Am. Chem. Soc.* **2008**, *130*, 7496−7502.
(39) Zhu, J.; Ferrer, N.; Hayward, R. C. *Soft Matter* **2009**, *5*, 2471−2478.
(40) Yu, H.; Jiang, W. *Macromolecules* **2009**, *42*, 3399−3404.
(41) Betthausen, E.; Hanske, C.; Müller, M.; Fery, A.; Schacher, F. H.; Müller, A. H. E.; Pochan, D. J. *Macromolecules* **2014**, *47*, 1672−1683.
(42) Lund, R.; Willner, L.; Richter, D.; Lindner, P.; Narayanan, T. *ACS Macro Lett.* **2013**, *2*, 1082−1087.
(43) Han, Y.; Yu, H.; Du, H.; Jiang, W. *J. Am. Chem. Soc.* **2010**, *132*, 1144−1150.
(44) Yang, S.; Yu, X.; Wang, L.; Tu, Y.; Zheng, J. X.; Xu, J.; Van Horn, R. M.; Cheng, S. Z. D. *Macromolecules* **2010**, *43*, 3018−3026.
(45) Ma, Q. G.; Remsen, E. E.; Clark, C. G.; Kowalewski, T.; Wooley, K. L. *Proc. Natl. Acad. Sci. U.S.A.* **2002**, *99*, 5058−5063.
(46) Granek, R. *Langmuir* **1996**, *12*, 5022−5027.
(47) Sammalkorpi, M.; Karttunen, M.; Haataja, M. *J. Am. Chem. Soc.* **2008**, *130*, 17977−17980.
(48) Ryu, C. Y.; Lodge, T. P. *Macromolecules* **1999**, *32*, 7190−7201.
(49) Bendejacq, D.; Joanicot, M.; Ponsinet, V. *Eur. Phys. J. E* **2005**, *17*, 83−92.
(50) Sota, N.; Saijo, K.; Hasegawa, H.; Hashimoto, T.; Amemiya, Y.; Ito, K. *Macromolecules* **2013**, *46*, 2298−2316.
(51) Nichols, F. A.; Mullins, W. W. *Trans. Met. Soc. AIME* **1965**, *233*, 1840−1848.
(52) Nose, T.; Iyama, K. *Comput. Theor. Polym. Sci.* **2000**, *10*, 249−257.
(53) Tan, H.; Wang, Z.; Li, J.; Pan, Z.; Ding, M.; Fu, Q. *ACS Macro Lett.* **2013**, *2*, 146−151.
(54) Geng, Y.; Discher, D. E. *Polymer* **2006**, *47*, 2519−2525.
(55) Oltra, N. S.; Swift, J.; Mahmud, A.; Rajagopal, K.; Loverde, S. M.; Discher, D. E. *J. Mater. Chem. B* **2013**, *1*, 5177−5185.
(56) Jiang, J. Q.; Tong, X.; Morris, D.; Zhao, Y. *Macromolecules* **2006**, *39*, 4633−4640.
(57) Zhang, H.; Xia, H.; Wang, J.; Li, Y. *J. Controlled Release* **2009**, *139*, 31−39.